Journal of Applied Physics

Environmental dependence of the photochromic effect of oxygen-containing rare-earth metal hydrides

Cite as: J. Appl. Phys. **129**, 153101 (2021); https://doi.org/10.1063/5.0041487
Submitted: 23 December 2020 . Accepted: 26 March 2021 . Published Online: 16 April 2021

Dmitrii Moldarev, Levin Stolz, Marcos V. Moro, Sigurbjörn M. Aðalsteinsson, Ioan-Augustin Chioar, Smagul Zh. Karazhanov, Daniel Primetzhofer, and Max Wolff

Journal of Applied Physics ARTICLE scitation.org/journal/jap

Environmental dependence of the photochromic effect of oxygen-containing rare-earth metal hydrides

Cite as: J. Appl. Phys. **129**, 153101 (2021); doi: 10.1063/5.0041487
Submitted: 23 December 2020 · Accepted: 26 March 2021 ·
Published Online: 16 April 2021

Dmitrii Moldarev,[1,2,3,a] Levin Stolz,[1] Marcos V. Moro,[1] Sigurbjörn M. Aðalsteinsson,[1] Ioan-Augustin Chioar,[1] Smagul Zh. Karazhanov,[2,3] Daniel Primetzhofer,[1] and Max Wolff[1,2]

AFFILIATIONS

[1]Department of Physics and Astronomy, Uppsala University, Box 516, 751 20 Uppsala, Sweden
[2]Department of Materials Science, National Research Nuclear University (MEPhI), Kashirskoe shosse 31, 115409 Moscow, Russia
[3]Department for Solar Energy, Institute for Energy Technology, 2027 Kjeller, Norway

[a)]**Author to whom correspondence should be addressed:** Dmitry.Moldarev@physics.uu.se

ABSTRACT

We study the dependence of the photochromic effect on environment and triggering light. We demonstrate that the first darkening/bleaching cycle of freshly grown films is accompanied by a release of weakly bound hydrogen, most likely present at the grain boundaries. For consecutive photochromic cycles, we do not find further exchange of material with the environment. Moreover, we report bleaching kinetics dependent on the gas environment after darkening with light of energies below the optical bandgap of the film. For darkening with photon energies above the bandgap of the film, we report a linear relation between the degree of darkening and bleaching relaxation time irrespective of gas environment.

I. INTRODUCTION

Metal hydrides are often used as catalysts or reducing agents[1] and battery materials,[2,3] but they have a strong tendency to oxidize and therefore are typically covered with a protective layer. It has been demonstrated that oxygen-containing yttrium hydride thin films are photochromic in air, i.e., reversibly change their absorption spectrum under illumination.[4] Later, a photochromic effect was also confirmed for scandium, dysprosium, gadolinium, erbium, and neodymium oxygen-containing hydrides.[5,6]

Photochromism is observed in a composition range δ (oxygen to yttrium ratio) between 0.5 and 1.5, with the sample composition following the overall non-stoichiometric equation: $MeH_{2-\delta}O_{\delta}$.[6,7] Based on charge neutrality considerations assuming single-phase metal oxyhydrides,[8,9] Cornelius *et al.*[10] proposed a different formula ($MeH_{3-2\delta}O_{\delta}$). Both these studies agree on the composition range in which photochromism is found. However, the typically columnar structure of the films suggests lateral concentration fluctuations, and indeed a more detailed and atomically resolved compositional analysis study using atom probe tomography and energy-dispersive x-ray spectroscopy revealed the presence of two phases (hydrogen- and oxygen-enriched, respectively) for a photochromic GdHO film.[11]

Photochromic films are commonly produced by depositing the rare earth metal dihydride either by reactive sputtering under an argon/hydrogen atmosphere[12] or by e^--beam evaporation.[13] The resulting MeH_2 (Me=Y, Gd, Dy, Sc, Er, or Nd) is subsequently oxidized in air. A polycrystalline columnar structure observed by transmission electron microscopy[11] facilitates oxidation and ensures a uniform distribution of oxygen atoms throughout the whole thickness of the film.[14] The performance of the photochromic films strongly depends on the microstructure and porosity as these parameters critically influence the oxidation behavior.[14] Films, which are kept in air, develop from opaque metal hydride over photochromic oxygen-containing metal hydride into transparent metal oxide.

Despite intensive studies of these materials over the last decade, the mechanism behind the photochromic effect remains disputable. *In situ* composition analysis under photodarkening and bleaching revealed no changes in composition larger than the sensitivity of the method that is limited by statistical uncertainty and on

the order of one atomic percent.[15] On the other hand, x-ray diffraction studies showed a reversible shift of the powder diffraction peaks toward larger Q values under illumination.[16,17] Moreover, the authors observed that substantial bleaching was only found under exposure to air but not in nitrogen atmosphere and concluded that the films may breathe oxygen. However, a closer look at the diffraction data shows that the apparent shift of diffraction peaks may be explained by material transport between the sub-phases rather than with the environment. The Bragg reflections of the oxide and hydride phases are very close to each other (see, for instance, ICDD powder diffraction files 00-050-1107 and 00-012-0797). Thus, the diffracted intensity may just be redistributed among these two phases, e.g., hydrogen and/or oxygen may migrate between the subphases resulting in the photochromic effect as it was reported in a pressurized photochromic yttrium foil.[18] This theory is further supported by Remhof *et al.*[19] who showed that tiny changes in hydrogen concentration, in the range from $YH_{1.9}$ (higher transmission) to $YH_{2.1}$ (lower transmission), in the fcc, β-phase go in hand with strong relative changes in optical transmission.

In this article, we shed further light on the role of material exchange with the environment. We investigate the darkening and bleaching kinetics of oxygen-containing rare earth metal hydrides in different gas environments. We show that samples darkened for the first time release hydrogen under illumination. Moreover, we demonstrate that the dependency of bleaching on gas environment is only found if the films are darkened with photons of energy smaller than the bandgap but not for photons of energy larger than the bandgap.

II. EXPERIMENTAL DETAILS

Dysprosium and yttrium hydride films were produced by reactive magnetron sputtering in Ar:H_2 atmosphere on a soda-lime substrate (microscope slides, $10 \times 10\,mm^2$ and 1 mm thick) and oxidized in air. Commercially available Dy and Y targets (with nominal purity of 99.99% and 99.9%, respectively) were used, and the target-substrate distance was varied from 4 to 8.5 cm. The plasma sputtering current was 120 mA without intentional heating of the substrate. For further details regarding sample preparation, we refer the reader to Ref. 6.

The chemical compositions and thicknesses of the resulting photochromic films were extracted from iterative and self-consistent ion beam analysis (IBA), combining Rutherford backscattering spectrometry, coincidence time-of-flight energy elastic recoil detection analysis, and nuclear reaction analysis. For the measurements, 2 MeV $^4He^+$, 36 MeV $^{127}I^{8+}$, and 6.4–6.7 MeV $^{15}N^{2+}$ ions were used as probing beams, respectively. More details on the composition analysis of photochromic oxygen-containing rare earth metal hydride films can be found elsewhere.[6,15]

Transmission spectra of the samples were measured using a Perkin Elmer Lambda 35 UV/Vis spectrophotometer and normalized to the transmission of air. The photochromic response, ΔT, is defined as the relative change of averaged optical transmission before and after illumination (integrated over the wavelengths' interval between 500 and 900 nm). The effect of wavelength and intensity on photodarkening and bleaching in air was studied using an in-house-developed modular optical diffractometer (see Fig. S1 in the supplementary material), equipped with a supercontinuum laser (SC Fianium SC-400-2) delivering light in the wavelength range from 370 to 2600 nm. The output of the light source is coupled to a dual acousto-optic tunable filter (AOTF) acting as a monochromator with a bandwidth of 2–5 nm for the visible (AOTF VIS 400–760 nm) and near-IR ranges (AOTF NIR 550–1100 nm). The AOTF NIR capable to provide eight different wavelengths simultaneously was used as probing light, whereas one specific wavelength delivered by AOTF VIS was utilized for photodarkening. The probing light was splitted by a beam splitter, and both beams were detected using Si photodiodes (Thorlabs DET100A) and lock-in detection, allowing for on-the-fly normalization of transmittance. To measure transmittance averaged over the VIS-NIR part of the spectrum, the following wavelengths were used as probing light: 520, 560, 600, 640, 680, 720, 760, and 800 nm. To minimize possible parasitic photodarkening from probing light, its intensity was optimized by measuring transmittance over time. A continuously variable neutral-density filter (Thorlabs NDC-50C-4M) was installed to modulate the intensity of the triggering light.

Bleaching in different environments was studied using a vacuum chamber connected to a turbo-molecular pump and equipped by two view ports allowing for a measurement of optical transmittance. A SPECTRA satellite residual gas analyzer was installed at the inlet of the turbo pump to monitor changes in gas composition.

All samples studied in this paper are summarized with their respective composition, δ, direct optical bandgap, E_g^{dir}, as extracted from Tauc plots[20] (see Fig. S2 in the supplementary material), and thickness, D, in Table I. The film thicknesses in nanometers were deduced from IBA assuming bulk densities; for details, see Ref. 21. The oxygen and hydrogen concentrations, δ and $2-\delta$, respectively, follow the composition suggested in Ref. 7.

TABLE I. Photochromic films investigated in this study. D and Y symbolize dysprosium- and yttrium-based films. Values for samples YI and YIII are taken from Refs. 7 and 15, respectively.

Notation	δ	E_g^{dir} (eV)	D (nm)
DI	1.04	2.84	630
YI	0.68	2.83	780
YII	1.15	2.83	1773
YIII	0.77	2.86	790

III. RESULTS

Figure 1(a) depicts the transmission spectrum of sample YI in the transparent state together with the spectra of light from the AOTF VIS used for photodarkening in air. Photochromic response $\Delta T_{darkening}$ and bleaching $\Delta T_{bleaching}$ for different transparency levels of the neutral-density filter and thereby for different intensities of triggering light ($\lambda = 430$ nm) are presented in Fig. 1(b). A nearly linear dependence is observed for both forward and backward reactions, which is typical for a single-photon process. The ratio between the two contrasts remains constant with a change in light intensity ($\Delta T_{darkening}/\Delta T_{bleaching} \approx 2$), indicating that the processes

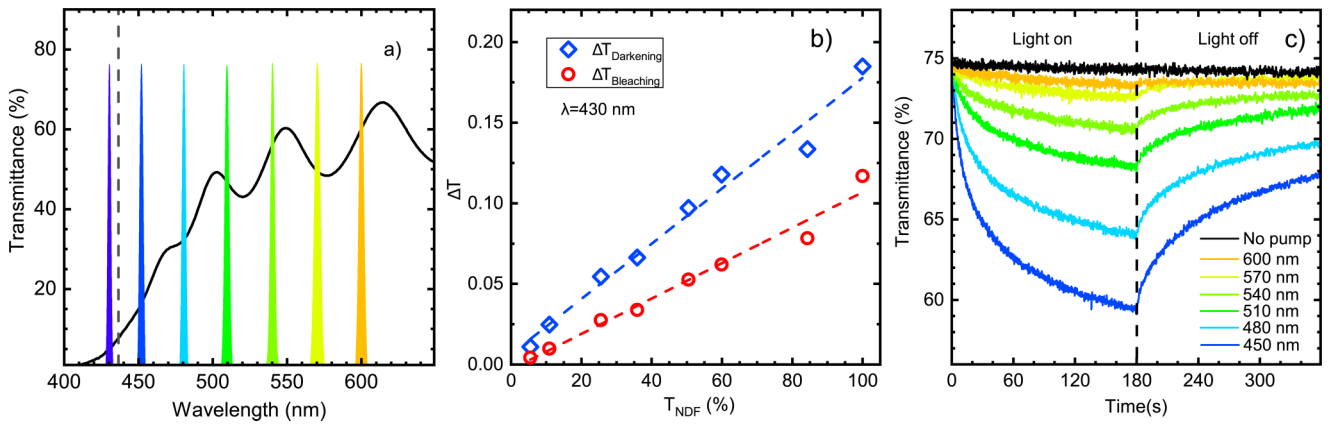

FIG. 1. Left panel (a): Transmission spectrum of sample YI plotted together with the wavelength from the super-continuum laser used for photodarkening in air. The dashed black line marks the wavelength corresponding to E_g^{dir} of the film. Central panel (b): ΔT after 180 s of photodarkening with 430 nm photons and after 180 s of bleaching plotted vs intensity. Blue and red dashed lines represent linear fits of $\Delta T_{darkening}$ and $\Delta T_{bleaching}$, respectively. Right panel (c): Photodarkening and bleaching for different wavelengths plotted vs time.

of photodarkening and bleaching are coupled. The energy of the photons affects the photochromic reaction in a similar manner as their flux [see Fig. 1(c)]. The strongest/fastest photochromic effect is observed for light with a wavelength of 450 nm. The decrease in energy yields weakening of the response, which almost fully vanishes for orange light (600 nm). A similar trend of photochromic response decreasing for a longer wavelength was observed in Ref. 22. Note that the AOTF VIS delivers higher intensity for longer wavelength and photochromic response scales with the number of photons at a given wavelength [see Fig. 1(b)]. Using light sources of same intensity would yield the same trend, but the wavelength dependence would be even more significant.

To study the effect of gas exposure, sample YII was loaded into a vacuum chamber and exposed to blue light emitted from a LED-array with $\lambda = 455$ nm ($E = 2.72$ eV) and $W_{\text{flux}} \approx 500\ \text{mW cm}^{-2}$ and purple light with $\lambda = 400$ nm ($E = 3.1$ eV) and $W_{\text{flux}} \approx 10\ \text{mW cm}^{-2}$. Figure S3 in the supplementary material shows the optical transmission of sample YII together with the spectra of both light sources. While the wavelength of blue light is at the absorption edge of the film, the purple light is in a regime in which the sample is strongly absorbing. The same holds true for all samples studied in this work: the purple light (3.1 eV) and the blue light (2.72 eV) are above and below the band gap, respectively (see Table I).

Sample YII was photodarkened in high vacuum to the same level of $\Delta T \approx 0.23$, which took 4 h for the purple light and 33 min for the blue one, as a consequence of the different power of the light sources. The total energy of the purple light ($40\ \text{mWh cm}^{-2}$) is about seven times smaller as compared to the blue one ($275\ \text{mWh cm}^{-2}$) demonstrating again that light of a shorter wavelength is more efficient in photodarkening the films. Figure 2 shows the bleaching of the sample. It turns out that for the film darkened by purple light (slower darkening and lower total energy), the bleaching in HV is significantly faster.

In order to address a possible gas release and absorption during photodarkening and bleaching, we have done experiments on samples YII and DI inside an ultra-high vacuum (UHV) system. The photochromic films were darkened, while the composition of the gas was monitored by a residual gas analyzer (RGA), attached at the inlet of a turbo molecular pump. Such a measurement allows qualitative information on the composition and the amount of the released material. Figure 3 summarizes the results by plotting the partial hydrogen gas pressure detected by the RGA vs time during and after illumination. To exclude other sources of gas release, e.g., degassing from the chamber walls or the substrate, a series of background measurements were done with the substrate (orange closed

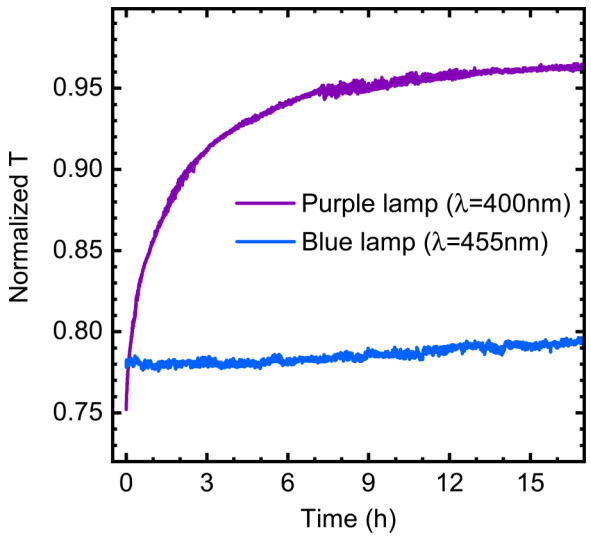

FIG. 2. Bleaching of sample YII in HV after photodarkening with purple (400 nm) light for 4 h and blue (455 nm) light for 33 min.

circles) only, no film deposited, and the empty chamber (red closed circles). No gas release was detected above 10^{-9} mbar, which is the sensitivity of the RGA.

Sample YII was illuminated with the blue LED directly after growth and photodarkened for the first time. During the first 5 min of illumination, the hydrogen partial pressure steeply raises to values of $\approx 2.1 \times 10^{-7}$ mbar, which is more than 400 times the base pressure. For times longer than 5 min, the partial hydrogen pressure decreases. After switching, the LED off the partial hydrogen pressure quickly drops to the base pressure. Considering a pumping speed of 170 L/s for H_2 and integrating pressure over the time of illumination, this results in 10^{16} hydrogen atoms, which is about 1% of the total hydrogen $\approx 10^{18}$, contained in the film. Note that for our estimate we assume that all gases in the chamber are extracted via the turbo pump.

To reproduce our results, we have repeated this experiment with sample DI and find qualitatively the same result. After the first photochromic cycle, films were exposed to air and then the experiment was repeated (green and blue stars). During the second darkening of the films, still a slight increase in hydrogen partial pressure is visible, however, at a much lower level than during the first cycle. Our results can be explained by assuming some of the hydrogen in the film, which is weakly bound and very mobile, becoming released under illumination. In parallel to the hydrogen release, we also detected a weaker release of O_2 and H_2O resulting in a 2.5 and 3.7 times (above base pressure) increased partial pressure, respectively, and indicating weakly bound O and possibly H_2O, with total quantities equivalent to sub-mono-layers. Note that both samples showed persistent photochromism after these two photodarkening cycles. Therefore, a significantly lower release of H_2 during the second cycle cannot be attributed to the degradation of the photochromic properties.

To check whether the hydrogen released from the film during photodarkening is reabsorbed during relaxation, we have done bleaching experiments in H_2 and in other environments like UHV, O_2, and technical air. The experimental procedure was as follows. Samples YII and DI were photodarkened in UHV by blue light. Then, the light was switched off, and the samples were exposed to different gases. Thereupon, the vacuum chamber was vented and the samples were bleached in air. Transmittance of the samples was monitored at every stage of bleaching. Figure 4 summarizes the results. The optical transmittance of samples YII and DI is plotted vs bleaching time. The bleaching process in UHV is, if it exists at all, very slow [see also Fig. 2(b)]. Exposure to pure O_2, pressure 1.5 bar (which is 7 times higher than the partial pressure of O_2 in air), and H_2 does not lead to substantial bleaching either, as seen in Figs. 4(a), 4(b), and 4(d). Figure 4(d) covers much longer bleaching times. A similar behavior of the YHO film was earlier reported in N_2 atmosphere.[17] Once the chamber is vented and the sample is exposed to air, however, the film bleaches quickly, which is especially evident from Figs. 4(a) and 4(d). Significant bleaching is also observed in technical/dry air [composition of technical air: N_2 + 20(1)% O_2, $H_2O < 3$ ppm, $C_nH_m < 0.1$ ppm, $CO < 1.0$ ppm, $CO_2 < 1.0$ ppm], containing mostly nitrogen and oxygen, both at pressures of 1 bar [see Fig. 4(c)]. In this case, subsequent venting of the chamber does almost not change the bleaching kinetics,

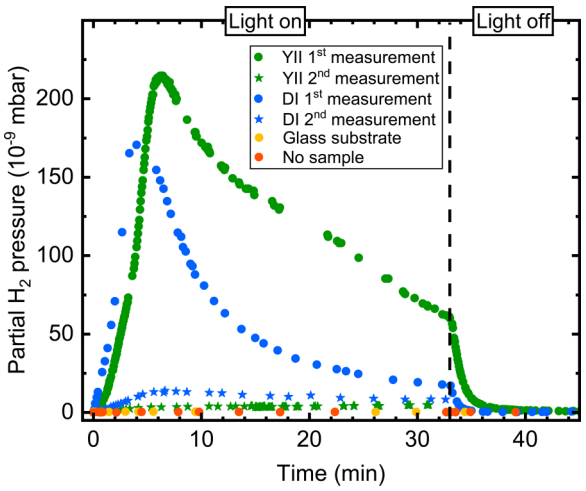

FIG. 3. Partial pressure of H_2 for photochromic films darkened with blue light (455 nm) in UHV. Both samples were darkened for the first time after production. The pressure drops rapidly toward the base pressure once the light source is switched off. During a second cycle of photodarkening, a significantly smaller gas release is found.

demonstrating that water, present in the ambient air, does not play a key role in the bleaching process.

The data in Fig. 2 show that the bleaching process in vacuum is depending on the wavelength used for photodarkening. To investigate this effect together with the gas release and re-absorption, we illuminated sample YIII for 4 h with purple light in UHV and studied the bleaching kinetics. Figure 5(a) depicts the transmission of the film plotted vs time under exposure to different gases. The bleaching follows an exponential increase in transmitted intensity, and a fit of the relaxation time [see Eq. (1) in supplementary material] shows that the sample bleaches on very similar time scales independent of environment: UHV, air, or H_2 ($\tau_{HV} = 1.87$ h, $\tau_{air} = 2.60$ h, $\tau_{H_2} = 2.76$ h).

To get a better handle on the bleaching kinetics, we have done systematic studies on sample YIII photodarkened in UHV to various degrees with purple light and subsequently exposed to different gases. Figure 5(b) summarizes the results. For films photodarkened to a photochromic response of up to about 22%–25%, the relaxation time is less than 3 h. For stronger darkening, the relaxation time linearly increases to about 18 h for photodarkening of about 42% again independent of the environment.

IV. DISCUSSION

Studies on bleaching in different environments show that the photochromic effect may be significantly different depending on the spectrum of the triggering light. For photodarkening in UHV with purple light, bleaching is almost independent of the gas environment. This situation completely changes when illuminating the films with blue light. In this case, we find a significant difference in bleaching times depending on whether bleaching is done in air and technical air or UHV, H_2, and O_2, indicating a possible material

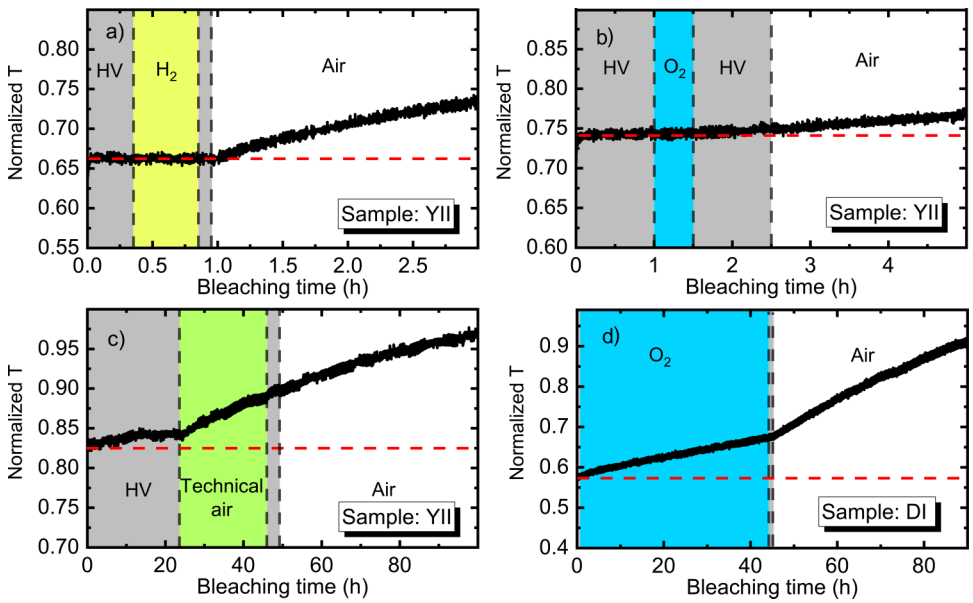

FIG. 4. Normalized optical transmission of YII (a), (b), (c), and DI (d) after photodarkening 33 min with blue light in HV plotted as a function of bleaching time in HV (gray), H_2 (yellow), and O_2 (blue) as well as technical gas (green) and air (white). The red dashed line illustrates transmission after illumination.

exchange with the environment. Besides, our results with blue light in different environments show a difference in bleaching kinetics (see Fig. S4 in the supplementary material). Studies of photochromic films capped by transparent layers acting as a diffusion barrier could shed more light onto possible photo-induced material transport.

The difference in bleaching for purple and blue light (i.e., for energies above and below bandgap, respectively) might be an indication that different photochromic processes are activated by different energies. Above a threshold of $\Delta T \approx 20\%$, we find a linear relation between the level of darkening and the relaxation time for bleaching irrespective of gas environment [see Fig. 5(b)]. Below this threshold, films bleach quickly and irrespective of the level of darkening.

At this point, the source of released H_2 remains unclear and may be originating from either the bulk of the film or as a product of photo-catalytic water splitting happening at the surface. The latter scenario is reported, for instance, for photochromic transition metal oxides,[23–26] which undergo a color change under proton injection from water molecules. Light-induced proton injection could also explain the lattice contraction under illumination:[16,17] H is located in the tetrahedral sites in $YH_{1.9}$, whereas an increase in H concentration up to $YH_{2.1}$ leads to a filling of octahedral sites, causing a compression of the crystal lattice.[27] The verification of this hypothesis goes beyond the scope of this paper but can be done by probing the local structure with EXAFS before and after illumination. The significantly lower RGA signal resulting from H_2 during the second cycle may be related to the so-called memory effect, i.e., accelerated photodarkening of the previously illuminated and bleached sample, reported in Ref. 4. The second illumination results in a faster photochromic response since part of the ions (e.g., protons) migrate between the subphases as proposed in

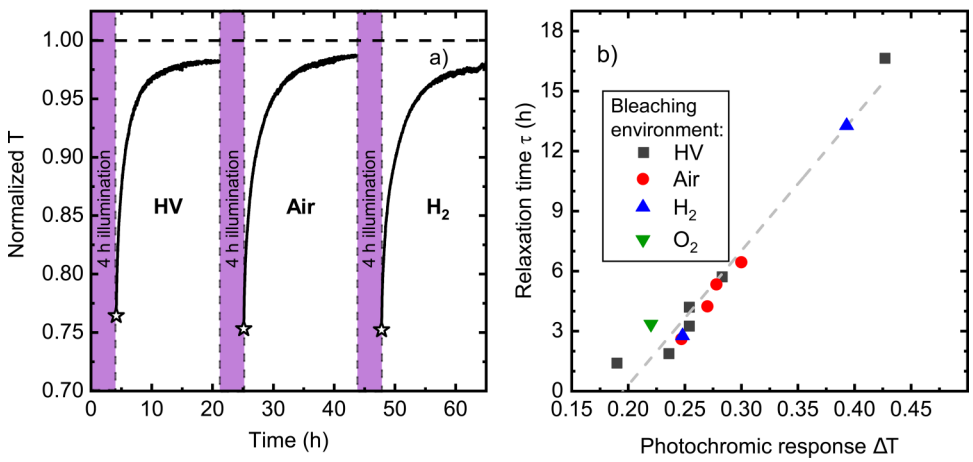

FIG. 5. Left panel (a): Optical transmission of YIII after photodarkening with purple light plotted vs time and bleached in UHV, H_2, and air. Right panel (b): Correlation between time constant τ for exponential bleaching in various atmospheres and photochromic response ΔT of sample YIII photodarkened in HV with purple light.

Refs. 11 and 18, and thus, no substantial gas release is observed. Nuclear magnetic resonance studies showed that 3% of hydrogen atoms are highly mobile and a corresponding signal of this species vanishes upon illumination, which can be related to H_2 release observed in the present work.[28]

V. SUMMARY AND CONCLUSIONS

We show that the photochromic effect is triggered by all wavelengths ranging from 400 to 600 nm used in the present study, even though some of them are of energies smaller than the bandgap of the sample. Light of shorter wavelength is more efficient for photodarkening as it results in larger photochromic contrast despite its lower intensity in comparison to the sources of longer wavelength. The photochromic response scales linearly with the number of photons, which indicates a single-photon nature of the effect. For photons with energies exceeding the bandgap of the film, we find bleaching that is independent of the environment, while films bleached at photon energies on the order of bandgap only bleach once exposed to air. Films photodarkened for the first time release detectable amounts of hydrogen, indicating material transport during photodarkening. Our results are in line with the assumption of hydrogen transport from the oxide to the hydride phase, which has the potential to explain the photochromic effect.

SUPPLEMENTARY MATERIAL

See the supplementary material for Figs. S1–S4 and Eq. (1).

ACKNOWLEDGMENTS

The authors thank Dr. Ayan Samanta for access to the spectrophotometer at the Department of Chemistry at Uppsala University and Dr. Vassilios Kapaklis for fruitful discussions. Accelerator operation is supported by the Swedish Research Council VR-RFI (Contract Nos. 821-2012-5144 and 2017-00646-9) and the Swedish Foundation for Strategic Research (Contract No. RIF14-0053). Dmitrii Moldarev thanks the Swedish Institute for the stipend for his research visit at Uppsala University granted as part of the Visby program. The Apollo setup is funded by the Knut and Alice Wallenberg Foundation project "Harnessing light and spins through plasmons at the nanoscale" (No. 2015.0060) and the Swedish Research Council (Project No. 2019-03581). The authors acknowledge FRINATEK Program of the Research Council of Norway (Contract No. 287545).

DATA AVAILABILITY

The data that support the findings of this study are available from the corresponding author upon reasonable request.

REFERENCES

[1]K. M. Waldie, F. M. Brunner, and C. P. Kubiak, "Transition metal hydride catalysts for sustainable interconversion of Co_2 and formate: Thermodynamic and mechanistic considerations," ACS Sustain. Chem. Eng. **6**, 6841–6848 (2018).
[2]Q. Cheng, D. Sun, and X. Yu, "Metal hydrides for lithium-ion battery application: A review," J. Alloys Compd. **769**, 167–185 (2018).
[3]J. W. Choi and D. Aurbach, "Promise and reality of post-lithium-ion batteries with high energy densities," Nat. Rev. Mater. **1**, 16013 (2016).
[4]T. Mongstad, C. Platzer-Björkman, J. P. Maehlen, L. P. Mooij, Y. Pivak, B. Dam, E. S. Marstein, B. C. Hauback, and S. Z. Karazhanov, "A new thin film photochromic material: Oxygen-containing yttrium hydride," Sol. Energy Mater. Sol. Cells **95**, 3596–3599 (2011).
[5]F. Nafezarefi, H. Schreuders, B. Dam, and S. Cornelius, "Photochromism of rare-earth metal-oxy-hydrides," Appl. Phys. Lett. **111**, 103903 (2017).
[6]S. Aðalsteinsson, M. V. Moro, D. Moldarev, S. Droulias, M. Wolff, and D. Primetzhofer, "Correlating chemical composition and optical properties of photochromic rare-earth oxyhydrides using ion beam analysis," Nucl. Instrum. Methods Phys. Res. Sect. B **485**, 36–40 (2020).
[7]D. Moldarev, M. V. Moro, C. C. You, E. M. Baba, S. Z. Karazhanov, M. Wolff, and D. Primetzhofer, "Yttrium oxyhydrides for photochromic applications: Correlating composition and optical response," Phys. Rev. Mater. **2**, 115203 (2018).
[8]H. Kageyama, K. Hayashi, K. Maeda, J. P. Attfiled, Z. Hiroi, J. M. Rondinelli, and K. R. Poeppelmeier, "Expanding frontiers in materials chemistry and physics with multiple anions," Nat. Commun. **9**, 772 (2018).
[9]H. Yamashita, T. Broux, Y. Kobayashi, F. Takeiri, H. Ubukata, T. Zhu, M. A. Hayward, K. Fujii, M. Yashima, K. Shitara, A. Kuwabara, T. Murakami, and H. Kageyama, "Chemical pressure-induced anion order–disorder transition in lnho enabled by hydride size flexibility," J. Am. Chem. Soc. **140**, 11170–11173 (2018), pMID: 30126273.
[10]S. Cornelius, G. Colombi, F. Nafezarefi, H. Schreuders, R. Heller, F. Munnik, and B. Dam, "Oxyhydride nature of rare-earth-based photochromic thin films," J. Phys. Chem. Lett. **10**, 1342–1348 (2019).
[11]M. Hans, T. T. Tran, S. M. Aðalsteinsson, D. Moldarev, M. V. Moro, M. Wolff, and D. Primetzhofer, "Photochromic mechanism and dual-phase formation in oxygen-containing rare-earth hydride thin films," Adv. Opt. Mater. **8**, 2000822 (2020).
[12]J. Montero, F. A. Martinsen, M. Lelis, S. Z. Karazhanov, B. C. Hauback, and E. S. Marstein, "Preparation of yttrium hydride-based photochromic films by reactive magnetron sputtering," Sol. Energy Mater. Sol. Cells **177**, 106–109 (2018).
[13]K. Kantre, M. V. Moro, D. Moldarev, M. Wolff, and D. Primetzhofer, "Synthesis and *in-situ* characterization of photochromic yttrium oxyhydride grown by reactive e-beam evaporation," Scr. Mater. **186**, 352–356 (2020).
[14]D. Moldarev, D. Primetzhofer, C. C. You, S. Z. Karazhanov, J. Montero, F. Martinsen, T. Mongstad, E. S. Marstein, and M. Wolff, "Composition of photochromic oxygen-containing yttrium hydride films," Sol. Energy Mater. Sol. Cells **177**, 66–69 (2018).
[15]M. V. Moro, D. Moldarev, C. You, E. Baba, S. Karazhanov, M. Wolff, and D. Primetzhofer, "*In-situ* composition analysis of photochromic yttrium oxyhydride thin films under light illumination," Sol. Energy Mater. Sol. Cells **201**, 110119 (2019).
[16]J. P. Maehlen, T. T. Mongstad, C. C. You, and S. Karazhanov, "Lattice contraction in photochromic yttrium hydride," J. Alloys Compd. **580**, S119–S121 (2013).
[17]E. M. Baba, J. Montero, E. Strugovshchikov, E. O. Zayim, and S. Karazhanov, "Light-induced breathing in photochromic yttrium oxyhydrides," Phys. Rev. Mater. **4**, 025201 (2020).
[18]A. Ohmura, A. Machida, T. Watanuki, K. Aoki, S. Nakano, and K. Takemura, "Photochromism in yttrium hydride," Appl. Phys. Lett. **91**, 151904 (2007).
[19]A. Remhof, J. W. J. Kerssemakers, S. J. van der Molen, R. Griessen, and E. S. Kooij, "Hysteresis in yh_x films observed with *in situ* measurements," Phys. Rev. B **65**, 054110 (2002).
[20]J. Tauc, R. Grigorovici, and A. Vancu, "Optical properties and electronic structure of amorphous germanium," Phys. Status Solidi B **15**, 627–637 (1966).
[21]D. Moldarev, M. Wolff, E. M. Baba, M. V. Moro, C. C. You, D. Primetzhofer, and S. Z. Karazhanov, "Photochromic properties of yttrium oxyhydride thin films: Surface versus bulk effect," Materialia **2**, 100706 (2020).
[22]C. C. You and S. Z. Karazhanov, "Effect of temperature and illumination conditions on the photochromic performance of yttrium oxyhydride thin films," J. Appl. Phys. **128**, 013106 (2020).
[23]T. He and J.-N. Yao, "Photochromism in transition-metal oxides," Res. Chem. Intermed. **30**, 459–488 (2004).

[24]T. He and J. Yao, "Photochromism of molybdenum oxide," J. Photochem. Photobiol. C **4**, 125–143 (2003).
[25]T. He and J. Yao, "Photochromic materials based on tungsten oxide," J. Mater. Chem. **17**, 4547–4557 (2007).
[26]A. Gavrilyuk, "Photochromism in WO_3 thin films," Electrochim. Acta **44**, 3027–3037 (1999).
[27]J. N. Daou and P. Vajda, "Hydrogen ordering and metal-semiconductor transitions in the system yh_{2+x}," Phys. Rev. B **45**, 10907–10913 (1992).
[28]C. V. Chandran, H. Schreuders, B. Dam, J. W. G. Janssen, J. Bart, A. P. M. Kentgens, and P. J. M. van Bentum, "Solid-state NMR studies of the photochromic effects of thin films of oxygen-containing yttrium hydride," J. Phys. Chem. C **118**, 22935–22942 (2014).